



STRUCTURAL, MORPHOLOGY AND PHOTOLUMINESCENCE PROPERTIES OF CERIUM DOPED ZINC OXIDE NANOPARTICLES PREPARED BY CO – PRECIPITATION METHOD

C.SELVARAJU¹, R.KARTHICK² & A.JUDITH JAYARANI³

¹PG and Research Department of Physics, H H The Rajah's College (Autonomous), Pudukkottai-622 001, India.

²PG & Research Department of Physics, National College (Autonomous), Tiruchirappalli-620 001, India.

³Assistant Professor, PG & Department of Physics, Bishop Heber College (Autonomous), Tiruchirappalli, 620017, India.

Abstract

Pure and Ce doped ZnO nanoparticles were synthesized by means of co-precipitation method. The structural analyses were done by X-ray diffraction (XRD) and it is several that the synthesized nanoparticles were well-crystalline and having hexagonal wurtzite structure of undoped ZnO and the nearness of Ce doped ZnO samples. The ascertained the normal crystallite measure from 27 to 42 nm with increment in Ce concentration. FESEM images delineated hexagonal shaped in ZnO nanoparticles. EDX affirms the synthesis of undoped and Ce doped ZnO nanoparticles. PL spectra affirmed that the intensityful Ce doping upgrades the visible emissions and smothers close band gap emission. The antibacterial effectiveness of Ce doped ZnO nanoparticles were explored against a Gram positive (*Staphylococcus aureus*) and Gram negative bacteria (*E.Coli*).

Keywords: Cerium; ZnO nanoparticles; Photoluminescence; FE-SEM; Antibacterial activity; Co – Precipitation method.

1.INTRODUCTION

Semiconductor nanomaterials have pulled in much consideration amid the previous couple of decades. The intrigue is because of its crucial research application, because of one of a kind size and shape subordinate optical, electrical, magnetic, photocatalytic, biomedical properties [1– 14]. Among them, ZnO nanomaterials with hexagonal wurtzite structure is outstanding n-type (II-IV) semiconductor with a wide band gap (3.37 eV) and substantial exciton binding energy of 60 meV [15– 17]. Inferable from these one of a kind properties, ZnO nanomaterials are showing adaptable applications in different fields [18]. Among the other rare earth (RE) doped particles have a few points of interest like simple joining into ZnO crystal which upgrades their application [19, 20]. For the RE-doped ZnO nanocrystals, they are relied upon to be potential candidate materials for flat panel shows because of their probability for efficiently emission in the visible range. Besides, ZnO is one of the ecological inviting materials, the RE-doped ZnO nanocrystals can likewise be utilized as fluorescence names for biological imaging. Up to this point, distinctive synthesis routes have been produced for the preparation of RE-doped ZnO nanostructures, for example, pulsed laser deposition, thermal dissipation, magnetron sputter deposition, pyrolysis, wet chemical etching, and chemical-cobstion process [21-28].

Cerium is a major component in the useful rare earth family. Up to now, there were restricted reports about fabrication of Ce-doped ZnO nanostructures [29, 30]. Deformities initiated by the doping and particularly the conceivable host electronic structure change after

doping impacts affect the optical properties of these nanoparticles. To the extent we known, small has been explored when Ce was doped into ZnO nanoparticles. So the structures, optical and electrical properties of Ce-doped ZnO nanoparticles still need additionally inquire about, which is vital for both basic and connected perspectives.

The co-precipitation technique allows mixing of the chemicals at atomic level, hence diminishing the likelihood of imperceptible impurity phases. Along these lines, in the present paper, Ce doped ZnO nanoparticles (NPs) have been synthesized by co-precipitation method which is a straightforward, simple to deal with, exceptionally compelling yet economical technique. Distinctive characterizations like X-ray diffraction (XRD) and field emission scanning electron microscope (FESEM) are performed for structural and morphological analysis. Energy dispersive analysis (EDX) spectrums for the nanoparticles have additionally been recorded for the ZnO phase affirmation. Besides, the accentuation on antibacterial activities of the synthesized Pure and Ce doped ZnO nanoparticles were tested against gram positive (*Staphylococcus aureus*) and gram negative (*E.Coli*) bacterial strains.

2. EXPERIMENTAL TECHNIQUES:

2.1. SYNTHESIS OF Ce – ZnO NANOPARTICLES

Undoped ZnO NPs is set up by getting 0.45M watery arrangement of Zinc Nitrate $Zn(NO_3)_2 \cdot H_2O$ and 0.9 M fluid solution of Sodium hydroxide (NaOH) are set up in distilled water. For Ce doped ZnO NPs, proper volume of 0.45 M solution of Cerium chloride is added

to 0.45M fluid solution of Zinc Nitrate to acquire 5, 10 and 15 at% doping of Ce. At that point NaOH solutions are warmed at the temperature around 55°C. The Zn(NO₃)₂.H₂O and Ce doped zinc nitrate solutions are one by one included drop shrewd (for 40 min.) to the NaOH solutions under high speed stirring respectively. The beakers are fixed at this condition for two hours. The precipitated undoped and Ce doped ZnO NPs are cleaned with deionized water and ethanol at that point dried in atmosphere at 60 °C. Hence there are four examples: undoped ZnO, ZnO: 3 at. % Ce, ZnO: 5 at. % Ce, and ZnO: 7 at.% Ce which are named as samples a, b, c and d separately. At that point, fluid solution of NaOH (3 M) was gradually included drop insightful into the solution under stirring at room temperature until the point that pH esteem was accomplished 12.

After 1 h, the solutions were matured and after that precipitates were gathered out for washing by ethanol and water separately to expel the unreacted reagents. The slurry was dried an oven at 80 °C for 10 h and tempered at 400 °C for 2 h.

2.2. CHARACTERIZATION:

X-ray diffraction (XRD) design was recorded at room temperature (PAN scientific X'Pert PRO with 2θ running from 5° to 80°, X-ray diffractometer utilizing CuKα irradiation (wavelength: 1.54056 Å)) X-ray source utilizing a current of 30 mA and a voltage of 40 kV. The surface of ZnO nanoparticles was dictated by FE-SEM images and composition (EDAX) of the example were seen by utilizing JEOL, JSM-67001. Room temperature Photoluminescence [PL] estimations were completed

utilizing JY Fluorolog-3-11 spectrometer.

2.3. ANTIBACTERIAL ACTIVITY:

Antibacterial activity was tested against both gram positive and additionally gram negative by disc diffusion method with small modifications. The 24 h bacterial cultures were swabbed in a Muller Hinton agar (MHA) altered plates. Whatmann filter paper (No.1) discs of 3 mm distance across were impregnated with 100 μL of the solution containing samples and these plates were permitted to dissipate for 1 h. Reference standard plates were set up with ampicillin (10 μg/mL) to think about the antibacterial activity of the samples. In the wake of drying, the discs were set in swabbed bacterial plates and hatched at 28 °C for 24 h. After brooding, plates were inspected for clear zone around the discs. An unmistakable zone in excess of 2 mm in diameter was taken for antibacterial activity.

3. RESULTS AND DISCUSSION:

3.1. STRUCTURAL STUDIES

Powder X-ray diffraction analysis was utilized to investigate the crystalline structure and phase purity of Pure and Ce doped ZnO nanoparticles. Figure 1 thinks about the powder XRD pattern of Pure and distinctive concentration levels of cerium into ZnO. The diffraction peaks observed for the precious crystal planes (1 0), (0 2) and (1 0 1) at 2θ = 32°, 34°, 36° affirmed the wurtzite hexagonal crystalline planes of ZnO (JCPDS No: 34-1451). The sharp diffraction peaks in the XRD pattern illustrate that ZnO is very crystalline in nature. Be that as it may, the increasing of doping concentration of Ce levels diminishes the intensity of diffraction peaks.

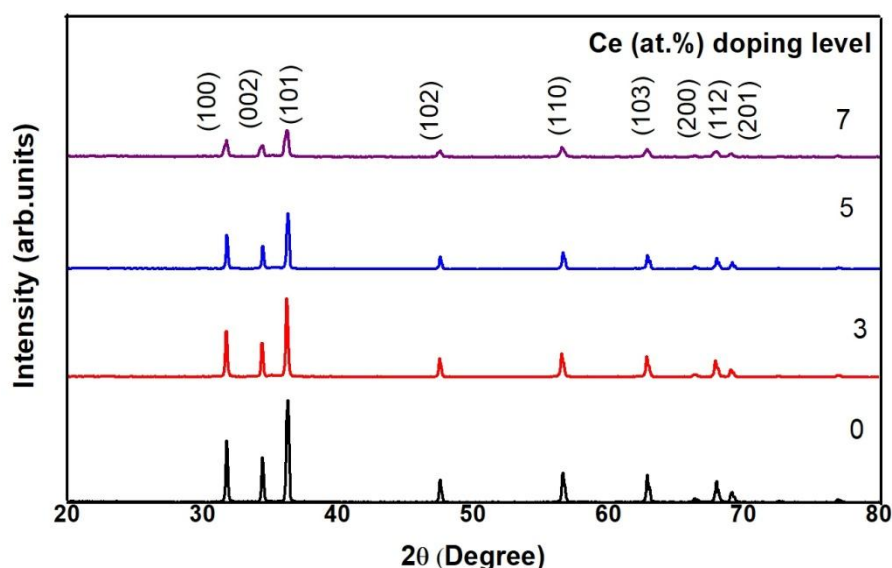


FIGURE 1
POWDER XRD PATTERN OF Ce DOPED ZnO NANOPARTICLES

The debasing of crystalline quality of ZnO proposes that the increase of doping concentration deteriorates the crystal structure. A small peak was

acquired at 2θ = 28.5° for the CZ1, CZ2, CZ3 test which is because of the nearness of higher centralization of cerium dopant in ZnO lattice section as indicated by the

JCPDS-No (75-0392) [31]. In the meantime, comes about show that move in peak positions towards higher 2θ happens due to the local strain caused by the doping of Ce^{3+} with a similarly bigger ionic radius (0.103 nm) supplanting the Zn^{2+} (0.074 nm) in ZnO lattice [32]. It is

observed that the widening of XRD peak of Ce doped examples lessen the size of ZnO nanoparticles. The normal crystallite size was evaluated by utilizing Scherrer formula as appeared in Table 1.

TABLE 1
STRUCTURAL PARAMETERS OF UNDOPED AND Ce DOPED ZnO NANOPARTICLES

Ce doping level (at.%)	D (nm)	*Lattice constants (Å)	
		a	c
0	42.04	3.270	5.211
2	35.79	3.256	5.218
4	31.59	3.258	5.220
6	27.60	3.260	5.223

(*Standard values: $a=3.2498 \text{ \AA}$, $c=5.2066 \text{ \AA}$ (JCPDS Card no. 36-1451).

2θ – Bragg's angle, D – Crystallite size)

$$D = K\lambda/\beta \cos\theta$$

(1)

Where, K is a shape constant (0.89), λ is the wavelength of X-ray (0.1540 nm), β is the full width at half most extreme and θ is the angle of diffraction. From the d separating values, the lattice constant 'a' and 'c' can be calculated by utilizing the Equation (2) and their values are introduced in Table 1.

$$1/d^2 = 4/3(h^2 + hk + k^2/a^2) + l^2/c^2 \quad (2)$$

Here h, k, l is the miller indices and dhkl speaks to the interplaner separating for indices (hkl).

The ascertained aspect ratio of Pure and Ce-doped samples is in great concurrence with the revealed estimation of 1.60 of ZnO. It affirms that the Ce^{3+} substituted Zn^{2+} ions in the overall crystal structure [33].

3.2. MORPHOLOGY AND ELEMENTAL COMPOSITIONS ANALYSIS:

Figure 2 demonstrates the FESEM images of undoped ZnO and Ce-doped ZnO nanoparticles. It can be seen that the undoped ZnO nanoparticles has a sharp tip-shaped like a needle. Moreover, the rod measurement is small with a normal of 125 nm. The ZnO nanoparticles with Cerium dopant is for the most part hexagonal fit as a fiddle with a normal distance across is sufficiently expansive around 340 nm. This marvel demonstrates that the cerium dopant impacts the direction and shape of the nanoparticles growth. This outcome was somewhat greater than the outcome got from similar techniques in past investigates which the distance across rod created were in the range of 100-200 nm.

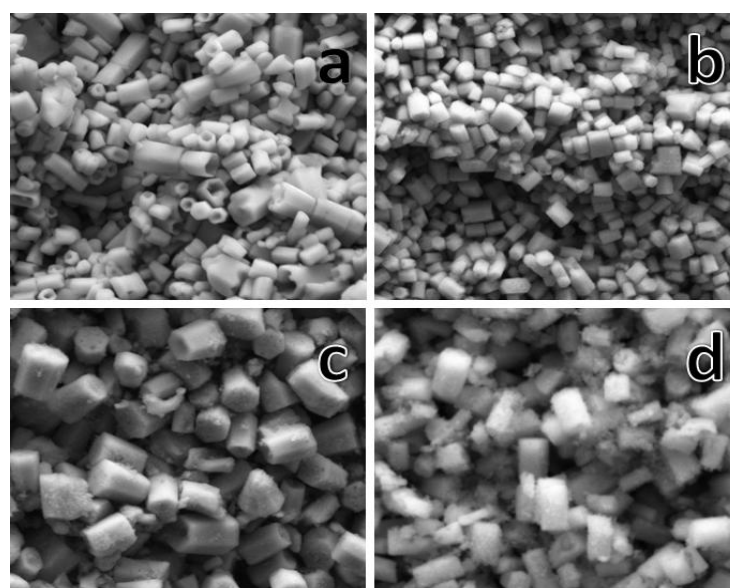


FIGURE 2
FESEM IMAGES OF Ce DOPED ZnO (a) 0 at.%, (b) 3 At.%, (c) 5 at.% AND (d) 7 at.% NANOPARTICLES

The elemental composition of Pure and Ce doped ZnO nanoparticles were inspected by EDX analysis Figure 3. The EDX analysis exhibited that Ce, Zn and O were just components display in the samples,

which affirm the presence of ZnO have structure. Therefore it was inferred that there were no impurities in the synthesized samples, which is connects with XRD results.

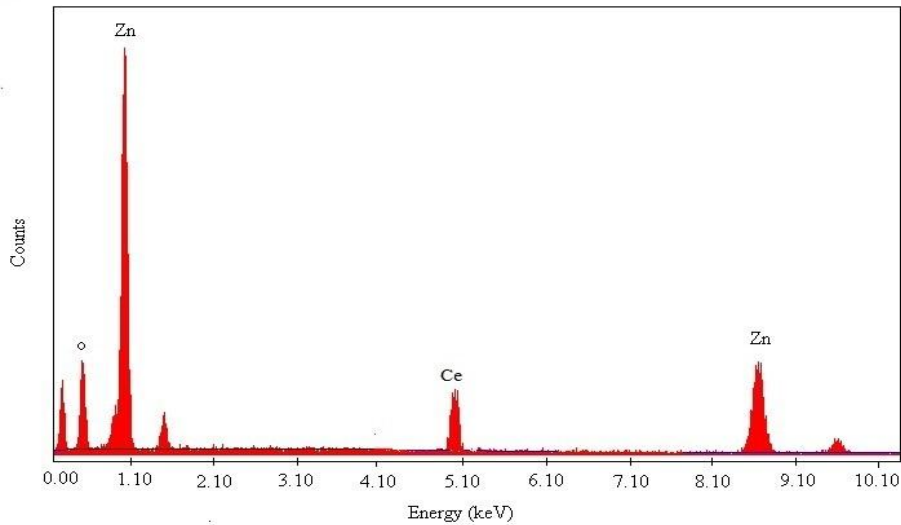


FIGURE 3
EDAX SPECTRA OF Ce (7at.%) DOPED ZnO NANOPARTICLE

3.3. PHOTOLUMINESCENCE SPECTRAL ANALYSIS

PL spectra of Pure and Ce doped ZnO nanoparticles were acquired by energizing with the radiation of wavelength 325 nm at room temperature as appeared in Figure 4. PL spectra demonstrate various

peaks in the range 390– 550 nm (both UV– Vis and Visible regions). A peak observed at 392 nm is ascribed to close band angle emission. A strong emission peak observed at 413 nm is because of the deformity states in the Ce doped ZnO nanoparticles, which might be oxygen vacancies.

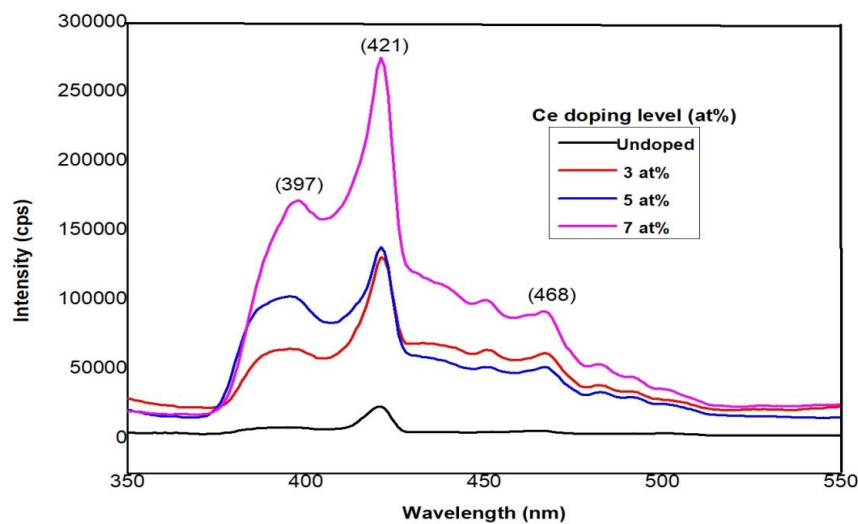


FIGURE 4
PHOTOLUMINESCENCE SPECTRA OF Ce DOPED ZnO NANOPARTICLES

The presence of emission band at 446 nm is ascribed to the progress from Zn interstitial to valence band while the blue emissions at 460 and 485 nm and the green emissions at 503, 527 and 541 nm are most presumably from the oxygen vacancies [34]. On doping Ce with ZnO, the peak's intensity diminish when compared with the Pure ZnO in the intensity of emission peaks. It is anticipated that the surface bound states go

about as deformity states prompting high non-radiative relaxation [35]. The low near band gap luminescence of Ce doped ZnO uncovers better restraint of pair obliteration and brought about UV extinguishing. These outcomes exhibit an awesome guarantee for tight band gap Ce doped ZnO nanoparticles with potential applications in optoelectronic devices.

3.4. ANTIBACTERIAL STUDIES

In present study, the relative antibacterial defenselessness of Pure and Ce doped ZnO nanoparticles towards a gram positive (G+) and a gram negative (G-) bacteria were studied in LB broth. Figure 5 (a) demonstrates the watched mean diameter restraint zones for Pure and Ce doped ZnO to dissect (G-) bacteria (E.Coli). The zones were increased as for the Ce dopant against the tested bacteria. While looking at the gram positive and gram negative, it has been watched that the

hindrance zone is higher in gram negative bacteria, this might be because of the distinction in their different structure and chemical composition of the cell surface. From these zone measurements, it could be expressed that Ce doped ZnO nanoparticles has successful antibacterial property, when contrasted with Pure ZnO nanoparticles. There are various instruments behind the antibacterial activity of metal oxide nanomaterials. Just a few of reports are accessible on account of antibacterial properties of doped ZnO.

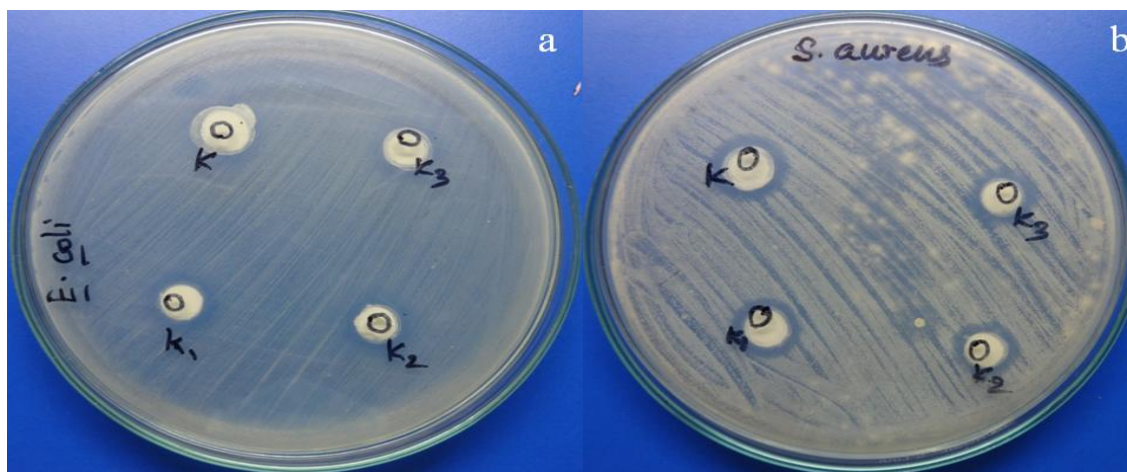


FIGURE 5
ANTIBACTERIAL ACTIVITY OF ZnO:Ce NANOPARTICLES AGAINST (a) E. coli AND (b) S. Aureus

Besides, unmistakably the antibacterial activity increments with diminish in particle size, because of the higher surface region of the samples. While contrasted with the wgap example, Pure ZnO had less antibacterial activity (Figure 6), while CZ3 had higher antibacterial activity identified with standard ampicillin Table 2. From the antibacterial test, it is affirmed that Ce doped ZnO nanoparticles render a compelling antibacterial operator,

when contrasted with Pure ZnO. It is likewise fascinating to take note of that both the samples have strong antibacterial activity against both a gram negative and a gram positive bacterial culture. Consequently, it could be presumed that the production of active species by photograph actuated response is the primary source towards bacterial harmfulness on account of doped metal oxide nanoparticles [36, 37].

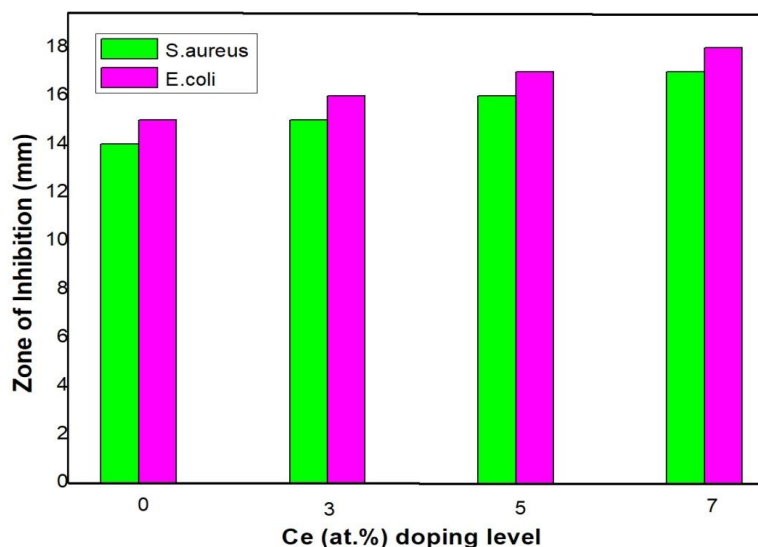


FIGURE 6
VARIATION IN THE ZONE OF INHIBITION CAUSED BY Ce DOPED ZnO NANOPARTICLES

4. CONCLUSION:

Pure and Ce doped ZnO nanoparticles were effectively synthesized co-precipitation technique. Powder XRD design displayed the wurtzite structure of samples. Hexagonal shaped nanoparticles like morphology were found for Pure and Ce doped ZnO, which was affirmed by FE-SEM studies. EDX investigation affirmed the nearness of Zn, O and furthermore demonstrated the nearness of Ce ions as an effective doped in ZnO. The antibacterial investigations against a gram positive and gram negative bacterial strains on Pure and Ce doped ZnO nanoparticles affirmed that the higher concentrations of Ce doped ZnO nanoparticles have an improved antibacterial impact than the lower concentration of Ce because of the oxygen opening identified with the electron – hole pairs of the nanoparticles.

REFERENCES

- Cui Y, Wang C, Wu S, et al, Cryst Eng Comm. 13, 4930–4934 (2011).
- Tankhiwale R, Bajpai S, Colloids and Surf B: Biointerfaces.90, 16–20 (2012).
- Dutta R, Nenavathu B, Talukdar S, Colloids Surf B: Biointerfaces.114, 218–224 (2014).
- Subramanian AP, Jaganathan SK, Manikandan A, et al, RSC Adv. 6, 48294–48314 (2016).
- Muthuvignesh V, Reddy VJ, Ramakrishna S, et al., RSC Adv.6, 83638–83655 (2016).
- Muthuvignesh V, Jaganathan SK, Manikandan A, RSC Adv. 6, 114859–114878 (2016).
- Meenatchi B, Velayutham Renuga, Manikandan A, The Korean J Chem Eng. 33, 934–944 (2016).
- Thilagavathi P, Manikandan A, Sujatha S, et al., Nanosci Nanotech Lett. 8, 438–443 (2016).
- Umopathy V, Manikandan A, Ramu P, et al., J Nanosci Nanotechnol.16, 987–993 (2016).
- Mathubala G, Manikandan A, Arul Antony S, et al., J Mol Struct.1113, 79–87 (2016).
- Umopathy V, Manikandan A, Arul Antony S, et al., Trans Nonferrous Met Soc China. 25, 3271–3278 (2015).
- Manimegalai DK, Manikandan A, Moortheswaran S, et al., J Supercond Novel Magn.28, 2755–2766 (2015).
- Mathubala G, Manikandan A, Arul Antony S, et al., Nanosci Nanotechnol Lett. 8, 375–381 (2016).
- Manikandan A, Hema E, Durka M, et al. J Inorg Organomet Polym Mater. 25, 804–815 (2015).
- Jandow NN, Yam FK, Thahab SM, et al., Curr. Appl Phys. 10, 1452–1455 (2010).
- Manikandan A, Vijaya J, Narayanan S, et al., J Nanosci Nanotechnol. 14, 2507–2514 (2014).
- Manikandan A, Judith Vijaya J, Ragupathi C, et al., J Nanosci Nanotechnol. 14, 2584–2590 (2014).
- Vijayaprasath G, Murugan R, Palanisamy S, et al., J Mater Sci: Mater Electron. 26, 7564–7576 (2015).
- Gao S, Zhang H, Deng R, et al., Appl Phys Lett. 89, 123125–123127 (2006).
- Teng XM, Fan HT, Pan SS, et al. J Appl Phys.100, 053507 (2006).
- J.-R. Duclère, B. Doggett, M. O. Henry, E. McGlynn, R. T. Rajendra Kumar, J.-P. Mosnier, A. Perrin, and M. Guilloux-Viry, J. Appl. Phys. 101, 013509 (2007).
- R. Pérez-Casero, A. Gutiérrez-Llorente, O. Pons-Y-Moll, W. Seiler, R. M. Defourneau, D. Defourneau, E. Millon, J. Perrière, P. Goldner, and B. Viana, J. Appl. Phys. 97, 054905 (2005).
- X. M. Teng, H. T. Fan, S. S. Pan, C. Ye, and G. H. Li, J. Appl. Phys. 100, 053507 (2006).
- J. S. John, J. L. Coffer, Y. Chen, and R. F. Pinizzotto, Appl. Phys. Lett. 77, 1635 (2000).
- M. Alaoui Lamrani, M. Addou, Z. Soofiani, B. Sahraoui, J. Ebothé, A. El Hichou, N. Fellahi, J. C. Bernède, and R. Dounia, Opt. Commun. 277, 196 (2007).
- Z. Sofiani, S. Bouchta, and M. Addou, J. Appl. Phys. 101, 063104 (2007).
- N. Mais, J. P. Reithmaier, A. Forchel, M. Kohls, L. Spanhel, and G. Müller, Appl. Phys. Lett. 75, 2005 (1999).
- Y. Liu, Q. Yang, and C. Xu, J. Appl. Phys. 104, 064701 (2008). Physica B 340, 235-239 (2003)
- B.Cheng, Y.Xiao, G. Wu, L. Zhang, Appl. Phys. Lett 84(3), 416-418 (2004)
- Kuzhalosai V, Subash B, Shanthi M, Mater Sci Semicond Proc. 27, 924–933 (2014).
- Kumari R, Sahai A, Goswami N, Structural, Prog Nat Sci: Mater Int. 25, 300–309 (2015).
- Kannadasan N, Shanmugam N, Cholan S, et al., Mater Charact. 97, 37–46 (2014).
- Qingzhi Wu, Xia Chen, Ping Zhang, et al., Cryst. Growth Des. 8, 3010–3018 (2008).
- Xu CX, Zhu GP, Li X, et al., J. Appl. Phys. 103, 094303 (2008).
- Chitra K, Reena K, Manikandan A, et al. J Nanosci Nanotechnol. 15:4984–4991 (2015).
- Chitra K, Manikandan A, Moortheswaran S, et al., Adv Sci Eng Med. 7, 710–716 (2015).

Figure captions

- Fig.1. Powder XRD pattern of Ce doped ZnO nanoparticles
 Fig.2. FESEM images of Ce doped ZnO (a) 0 at.%, (b) 3 at.%, (c) 5 at.% and (d) 7 at.% nanoparticles
 Fig.3. EDAX spectra of Ce (7at.%) doped ZnO nanoparticles
 Fig.4. Photoluminescence spectra of Ce doped ZnO nanoparticles
 Fig.5. Antibacterial activity of ZnO:Ce nanoparticles against (a) E. coli and (b) S.

aureus bacteria

Fig.6. Variation in the zone of Inhibition caused by Ce doped ZnO nanoparticles

Figure captions

Table 1. Structural parameters of undoped and Ce doped ZnO nanoparticles